

# The optical properties of bulk and (0 0 1) monolayer VS<sub>2</sub> based on first principles calculations

Jialun Li<sup>1,\*</sup>, Zhenyang Luo<sup>2</sup>, Jinge Hao<sup>3</sup>

<sup>1</sup>College of Science, Nanjing University of Science and Technology, Nanjing, Jiangsu, China

<sup>2</sup>School of Physics, Changchun University of Science and Technology, Changchun, Jilin, China

<sup>3</sup>School of Physics and Electronic Information, Henan Polytechnic University, Jiaozuo, Henan, China

\*Corresponding author

**Abstract:** VS<sub>2</sub> has a two-dimensional layered structure, possesses good catalytic activity as a vital member of the family of transition metal-sulfur compounds (TMDs), and it is an essential functional material for optoelectronics with a wide range of applications. While VS<sub>2</sub> with different structures possess different electronic structures and optical properties, this paper investigates their energy band structures, electronic properties, and optical properties based on density functional theory (DFT) with bulk VS<sub>2</sub> and (0 0 1) crystal-oriented monolayer VS<sub>2</sub> as the objects of study, respectively. According to the calculated results, the monolayer VS<sub>2</sub> has a smaller bandgap. It can effectively achieve ultra-broadband absorption, while there are also significant differences between the dielectric functions, absorption coefficients, and reflection coefficients of these two structures of VS<sub>2</sub>. Depending on these different properties and structures, these two structures of VS<sub>2</sub> could be used in different applications. These calculations provide theoretical support for the development of VS<sub>2</sub> optoelectronic materials and devices.

**Keywords:** VS<sub>2</sub>; first principles calculation; optical properties; first-principles

## 1. Introduction

Today, the energy demand is increasing. One of the most used energy sources is primary energy, which can only be extracted in minimal quantities. While functioning, they emit pollutants in various forms into the surrounding environment. Thus, it is why energy is one of the issues of great concern to all countries.

Semiconductor photocatalysis is a proven solution to the problem of environmental pollution and energy shortages. However, conventional photocatalytic materials have limited the further development of photocatalytic technology due to their wide bandgap [1] and low quantum efficiency. Therefore, there is a need to develop new photocatalytic materials.

Transition metal dichalcogenides (TMDCs) are considered one of the most promising photocatalytic materials due to their high photocatalytic activity. For example, MoS<sub>2</sub> shows high activity in photocatalytic hydrogen because of its ability to produce electron-hole pairs rapidly under excitation by light energy and its low potential for excited electrons in the conduction band [2] [3].

Today there are more than 60 types of TMDCs materials, two-thirds of which are layered. TMDCs can be expressed by the chemical formula MX<sub>2</sub>, where M stands for an over-metallic element and X for a sulfur group element. As a member of the TMDCs, VS<sub>2</sub> is an essential representative of new photocatalytic materials due to its diverse structural types, flexible and tunable physicochemical properties, and abundant and cheap sources. Most of them have potentially efficient photocatalytic properties, providing rich material for developing new photocatalytic materials. Due to structural differences, bulk and monolayer materials are often used in different applications. Although both are used in various applications, there is a lack of research into the photoelectronic differences between VS<sub>2</sub> monolayers and monoliths. Therefore, it is crucial to investigate their electrical and optical properties theoretically.

In order to investigate the electronic structure and related properties of the relevant monolayers and bulk VS<sub>2</sub>, this paper presents a comprehensive study of the fundamental physicochemical properties of bulk VS<sub>2</sub> and (0 0 1) monolayers based on density functional theory (DFT) to gain a clear understanding of the influence of the composition and crystal structure of VS<sub>2</sub> materials on their electronic structure

and optical properties. These studies provide references and theoretical support for the development of new sulfide photocatalytic materials and their heterostructure composite photocatalytic materials.

## 2. Calculation method and model

In this work, we obtain the initial model of  $\text{VS}_2$  from The Inorganic Crystal Structure Database (ICSD). For both the bulk and monolayer structures of  $\text{VS}_2$ , the CASTEP (Cambridge Serial Total Energy Package) [4] module in Materials Studio, based on density generalization theory, was used. In this, the core electrons (S: [Ne]) are treated with a super-soft pseudopotential, and the PBE [5] function in the generalized gradient approximation (GGA) is used to describe the generalized gradient correlation effect of the valence electrons S:  $3s_2 3p_4$ . The k-point sampling network for the Monkhorst-Pack method is  $5 \times 5 \times 2$  for the integrable Brillouin zone of the bulk  $\text{VS}_2$  and  $5 \times 5 \times 1$  for the Monkhorst-Pack method of the integrable Brillouin zone of the single-layer  $\text{VS}_2$ . For the bulk, we use a grid of  $18 \times 18 \times 81$  for the fast Fourier transform, while for the single-layer structure, we use a grid of  $18 \times 18 \times 120$  lattices for the fast Fourier transform. The minimization algorithm chosen for both lattice optimization is the BFGS (Broyden-Fletcher-Goldfarb-Shanno) [6] algorithm. The convergence criteria are as follows: the forces acting on the atoms should not exceed  $0.03 \text{ eV}/\text{\AA}$ , the stresses should not be greater than  $0.05 \text{ GPa}$ , the atomic displacements should not exceed  $0.001 \text{ \AA}$ , and the total energy change for each atom should be less than  $10^{-5} \text{ eV}$ . A Gaussian spread is applied to the eigenvalues calculated from CASTEP. The initial  $\text{VS}_2$  model used in this work was obtained from The Inorganic Crystal Structure Database (ICSD). Based on the optimized crystal structure, the electronic structure and optical properties of  $\text{VS}_2$  are further calculated. In order to obtain a monolayer  $\text{VS}_2$  model, the above-optimized bulk  $\text{VS}_2$  structure is first sliced in the (0 0 1) plane using the cleave surface function in material studio, and then a vacuum layer is created. The thickness of the vacuum layer was set to  $15 \text{ \AA}$  in order to avoid interactions between the different layers. Then the single  $\text{VS}_2$  layer was further optimized based on the above optimization criteria. Finally, calculations on the electronic structure and optical properties of the (0 0 1) surface crystalline  $\text{VS}_2$  are carried out.

## 3. Crystal structure

The crystal structures of the monolayers and bulks are shown in Figure 1.  $\text{VS}_2$  is a triangular structure in the present work, crystallizing in the hexagonal  $P6_3/mmc$  space group. The structure is two-dimensional and consists of two  $\text{VS}_2$  sheets facing in the (0 0 1) direction.  $\text{V}^{4+}$  is bonded to six equivalent  $\text{S}^{2-}$  atoms to form a shared-edge  $\text{VS}_6$  octahedron. All V-S bonds are  $2.36 \text{ \AA}$  long.  $\text{S}^{2-}$  is bonded to three equivalent  $\text{V}^{4+}$  atoms in a distorted t-shaped geometry.

After optimization, the lattice constants of the bulk  $\text{VS}_2$  are as follows:  $a=3.177502 \text{ \AA}$ ,  $b=3.177502 \text{ \AA}$ ,  $c=14.381435 \text{ \AA}$ . The lattice constants of the monolayer  $\text{VS}_2$  are as follows:  $a=3.18026 \text{ \AA}$ ,  $b=3.18026 \text{ \AA}$ ,  $c=14.42964 \text{ \AA}$ . The lattice constants of the monolayer  $\text{VS}_2$  are follows:  $a=3.18026 \text{ \AA}$ ,  $b=3.18026 \text{ \AA}$ ,  $c=14.42964 \text{ \AA}$ .

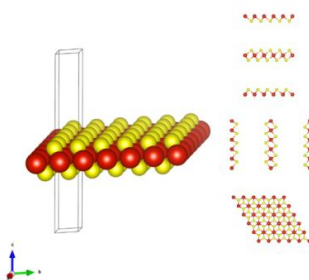


Figure 1: The crystal model of  $\text{MoSe}_2$  with different crystal structures. Red spheres represent V atoms and yellow spheres represent S atoms.

## 4. Electronic structure

### 4.1. Energy Band Structure

The energy band structure is also known as the electron energy band structure. In solid-state physics,

electrons are allowed or forbidden to carry a certain amount of energy due to the diffraction of quantum-dynamic electron waves in a periodic lattice. The band structure describes this feature. At the same time, the energy band of a material determines the number of other properties, particularly its electronic and optical properties.

We can classify solids as conductors, semiconductors, and insulators depending on the bandgap. Semiconductors can also be divided into direct and indirect bandgap semiconductors, depending on the energy band. For direct bandgap semiconductors, a semiconductor with the bottom of the conduction band and the top of the valence band located at the same point in k-space is called a direct bandgap semiconductor. In contrast, for indirect bandgap semiconductors, where the conduction band and valence band bottom are located at different points in k-space, the crossing direction shown on the energy band diagram is oblique; not only the direction of the crossing the energy but also the momentum is changed during the jump.

In order to compare the electronic structures of monolayer and bulk  $\text{VS}_2$ , we have calculated their energy band structures separately, as shown in Figure 2. For the bulk  $\text{VS}_2$ , since the bandgap is 0.624 eV, the valence-band maximum (VBM) is located at point G, while the conduction-band minimum (CBM) is located at one of points H and K. This means that the bulk  $\text{VS}_2$  is an indirect bandgap semiconductor. Also, since the bulk has a valence band top above 0, it exhibits specific metallic properties. For monolayer  $\text{VS}_2$ , the VBM is located at a point between points F and Q, while the CBM is located at a point between points F and G. This means that monolayer  $\text{VS}_2$  is also an indirect bandgap semiconductor with a calculated bandgap of 1.060 eV. Since the electrons in both structures of  $\text{VS}_2$  change their k-space position when they leap, there is a high chance of releasing energy to the lattice into phonons, which are released as thermal energy. Compared to bulk  $\text{VS}_2$ , monolayer  $\text{VS}_2$  exhibits good semiconductor properties as the electrons are more difficult to be excited from the valence band to the conduction band. At the same time, it has a lower intrinsic carrier concentration and lower electrical conductivity. At the same time, due to the nature of indirect bandgap semiconductors, monolayer  $\text{VS}_2$  requires momentum to complex with holes in the valence band, making it challenging to produce recombination-based luminescence. The narrow bandgap of both structures of  $\text{VS}_2$  results in good properties in terms of infrared light absorption. With these different characteristics of the surface layer and the bulk,  $\text{VS}_2$  has potential applications in optoelectronic switches.

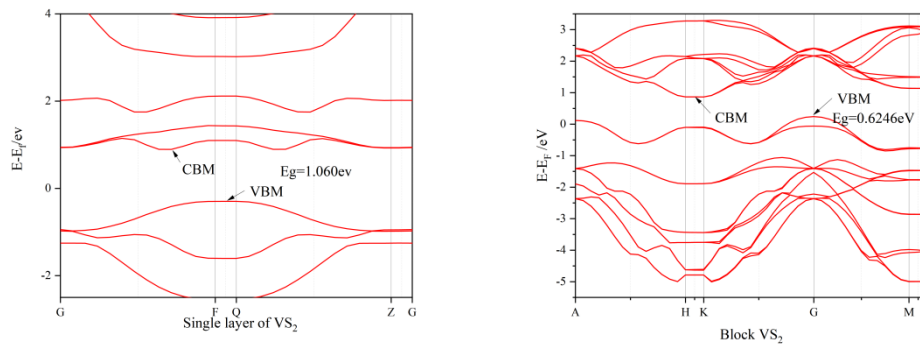


Figure 2: The calculated band structures of  $\text{VS}_2$  with two crystal structures

#### 4.2. Density of states

In order to investigate the chemical bonding mechanism of bulk and layered  $\text{VS}_2$ , their total density of states (DOS) and split-wave density of states (PDOS) are shown in Figure 3. From the total density of states plot, it can be seen that the valence bands of both structures are mainly distributed from -7 eV to 0 eV, and they are mainly composed of S-3p and V-3d. From the density of partial wave states, it can be seen that the S-3p electron has a sharp peak at -1.62 eV, forming a solid local state, which contributes more to the valence band than V-3d. The conduction band of  $\text{VS}_2$  for both structures is predominantly in the range of 0 eV to 4 eV and is composed mainly of S-3p and V-3d. As can be seen from the density of fractional wave states, the V-3d electrons of both structures have a sharp peak at 1.46 eV, forming a robust local state so that it makes a more substantial contribution to the conduction band than S-3p. Therefore, the electrical transport properties and carrier types of both structures  $\text{VS}_2$  are mainly determined by S-3p and V-3d.

Electrons in the lower energy regions of the Fermi energy level are the primary bonding electrons.

The greater the interaction between atoms, the higher the number of bonding electrons and the more stable the atoms for stable crystals. Integrating the total density of states between the Fermi energy levels near (-2 to 0 eV), the corresponding integrals for monolayer and bulk VS<sub>2</sub> are 0.4 and 0.87, respectively. Thus, the VS<sub>2</sub> stability of the bulk is more vital.

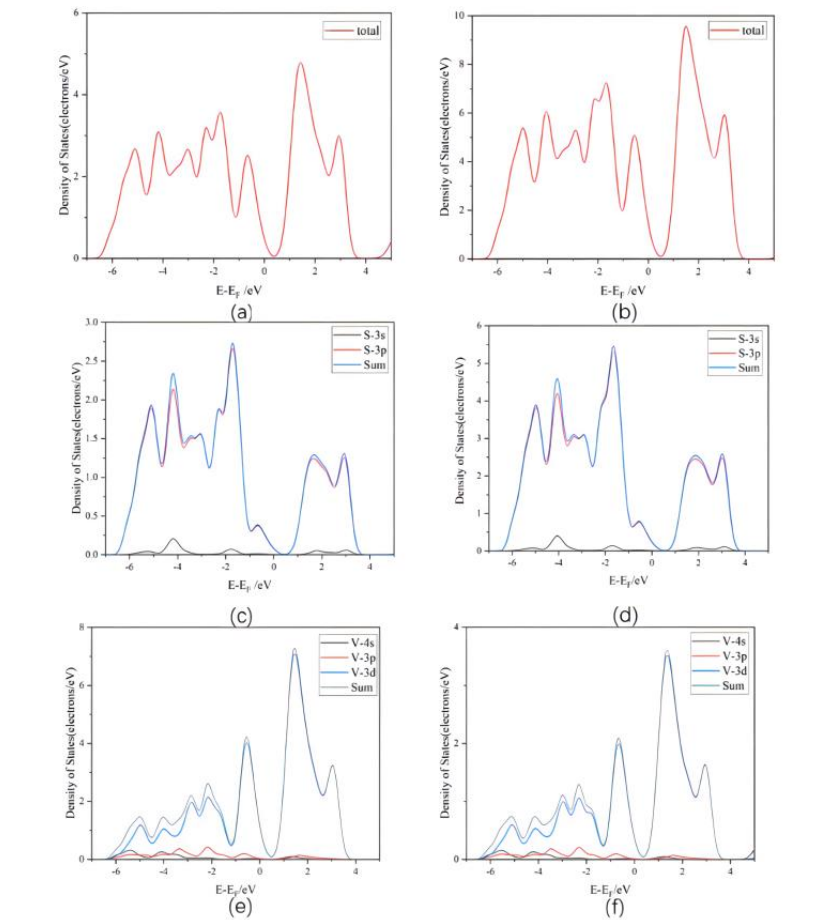


Figure 3: (a) Monolayer total density of states, (b) Bulk total density of states, (c) Monolayer S atomic density of states, (d) Bulk S atomic density of states, (e) Monolayer V atomic density of states, (f) Bulk V atomic density of states.

### 4.3. Dielectric functions

Dielectric functions  $\varepsilon(\omega) = \varepsilon_1(\omega) + i\varepsilon_2(\omega)$  known as the bridge between the microphysical processes of band-part leap and the electronic structure of a solid, when a single photon is irradiated on a crystalline material, the photon interacts with the electrons and ions in the crystal. However, due to the energy level structure, various linear or non-linear optical properties are displayed when an electron leap occurs. In the range of linear response, the complex permittivity function  $\varepsilon(\omega) = \varepsilon_1(\omega) + i\varepsilon_2(\omega)$  and the complex refractive index  $N(\omega) = n(\omega) + ik(\omega)$  have the following relationship:

$$\varepsilon_1 = n^2 - k^2$$

$$\varepsilon_2 = 2nk$$

The calculated real and imaginary parts of the curves of VS<sub>2</sub> for monolayers and bulks based on the electronic structure are shown in Figure 4. The calculated real and imaginary parts of the permittivity function of VS<sub>2</sub> for monolayers and bulks are shown in Figure 4. At low energies, the real part of the electron permittivity function increases with increasing energy, reaching a maximum for both structures at an energy of about 1.07 eV. However, the value of the monolayer VS<sub>2</sub> is relatively small compared to that of the bulk and then decreases with increasing energy. At energies of about 4 eV, the value of VS<sub>2</sub> for both structures is 0. From 0 to 4 eV, the value of the dielectric function of the bulk VS<sub>2</sub> is always about twice the value of the dielectric function of the monolayer VS<sub>2</sub> for the same energy. The imaginary

part of the dielectric function reflects the absorption properties of the material for photons. As can be seen from the graph, the wavelengths at which the peaks (imaginary part) of the bulk VS<sub>2</sub> are located are smaller than the wavelengths at which the peaks of the monolayer VS<sub>2</sub> are located. The peak of the imaginary part of the dielectric function is related to the electronic leap. According to the leaping rule and the peak matching the energy required for the leap, for both structures of VS<sub>2</sub>, the prominent peak of the dielectric function is attributed to the leap between the S-p electronic state in the valence band and the V-d energy level in the conduction band.

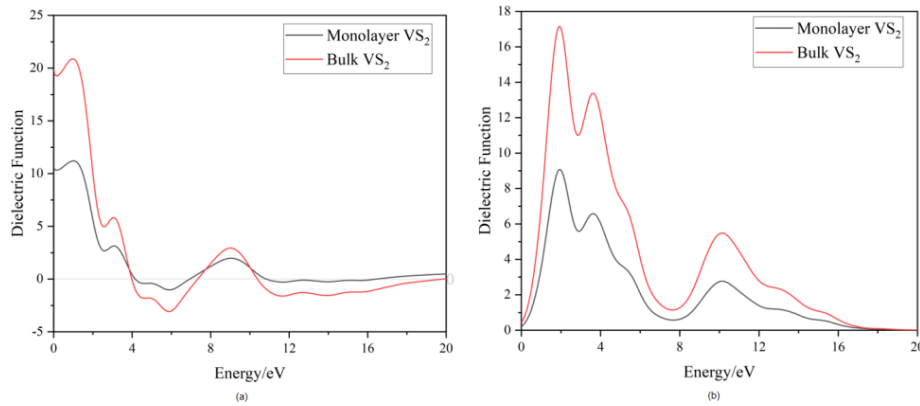


Figure 4: (a) Real part of the dielectric function, (b) Imaginary part of the dielectric function

#### 4.4. Refractive index

The refractive index of a solid is, where the real part  $n$  is the conventional refractive index and  $k$  is the extinction coefficient. In general, the larger the extinction coefficient, the greater the light absorption capacity of the solid. The real part  $n$  and the imaginary part  $k$  of the refractive index of VS<sub>2</sub> for both structures are shown in Figure 5. The reflectivity of the bulk VS<sub>2</sub> is significantly greater than the refractive index of the monolayer VS<sub>2</sub>. At wavelengths less than 1000 nm, the  $n$  part of the refractive index increases with increasing wavelength and then slowly decreases. The value of the  $k$  part of the bulk VS<sub>2</sub> is generally larger than that of the monolayer VS<sub>2</sub>. Therefore, we can conclude that the refractive index of VS<sub>2</sub> is related to the crystal structure and wavelength. The absorption capacity of the bulk VS<sub>2</sub> for light is larger than that of the monolayer VS<sub>2</sub>.

#### 4.5. Absorption and reflection coefficients

The reflection coefficient is the ratio of the intensity of light reflected from an object's surface to the intensity of the incident light when it hits the object. The reflection coefficient of an object receives a variety of factors, such as the angle of incidence of the incident light, its intensity, and the nature of the material on the object's surface. The reflection coefficient for the simple case of perpendicular incidence onto a plane can be obtained by matching the electric and magnetic fields on the plane:

$$R = \left| \frac{1 - N}{1 + N} \right|^2 = \frac{(n - 1)^2 + k^2}{(n + 1)^2 + k^2}$$

The absorption coefficient is the proportion of energy absorbed per unit length of light passing through an object and is generally used. In general, the absorption coefficient of a material is related to the type of material. However, the reflection and absorption coefficients of different structures of the same material are not necessarily the same, so analyzing the reflection and absorption coefficients of two structures of VS<sub>2</sub> material is essential for studying the optical properties of VS<sub>2</sub>.

Figure 5 shows the absorption and reflection spectra of these two structures of VS<sub>2</sub>. It is straightforward to see from the figure that the profiles of the light absorption curves of the two structures of VS<sub>2</sub> are very similar. Compared to the monolayer VS<sub>2</sub>, the bulk VS<sub>2</sub> shows a gradual redshift of the light absorption band edges. The bulk and monolayer VS<sub>2</sub> have good light absorption in the visible and infrared regions so that we can use them for photo detective materials, such as infrared sensors. The reflectance of VS<sub>2</sub> in both structures fluctuates considerably at wavelengths less than 1000 nm and gradually stabilizes after 1000 nm, making it suitable for use as an infrared optical detector. From the graph, we can also conclude that both structures of VS<sub>2</sub> show strong light reflectivity in both the visible and infrared regions so that their compound films can be used as antireflective layers with solid

applicability.

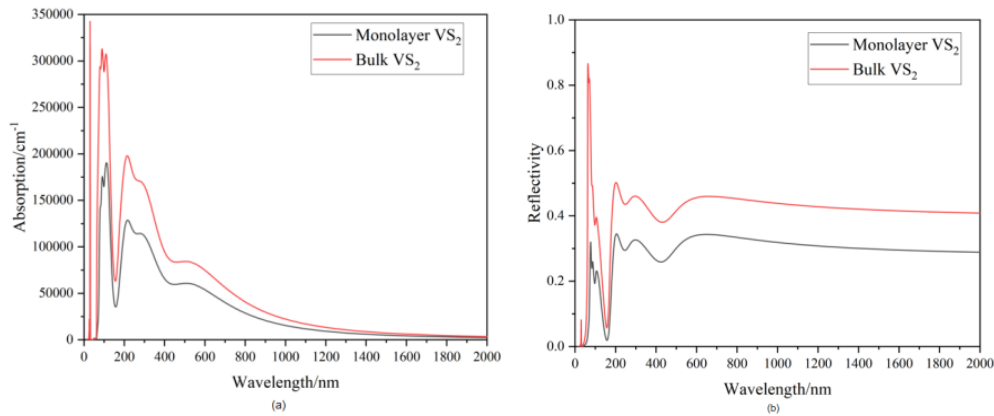


Figure 5: (a) Absorption spectrum of  $VS_2$  in two kinds crystal structures, (b) Reflection spectrum of  $VS_2$  in different crystal structures

The differences in the optical properties of bulk and monolayer  $VS_2$  are mainly attributable to differences in their crystal structures, which in turn lead to a change in their optical properties. At the same time, this difference in crystal structure leads to different interactions between the atoms and a change in the electronic structure. Theoretical calculations show that bulk  $VS_2$  has stronger ionic interactions and weaker covalent interactions between V and S atoms compared to monolayer  $VS_2$ . These data can provide reliable support for novel alum-based energy conversion materials and devices.

## 5. Conclusion

This thesis calculates the crystal structure, electronic structure, and optical properties of monolayer and bulk  $VS_2$  based on the DFT approach. Compared with monolayer  $VS_2$ , the bandgap of bulk  $VS_2$  is narrower. However, because they are essentially the same compound, many properties, such as the sharpness of the density of states peak, the variation of the bandgap, and the constituent electronic states at the top and bottom of the valence and conduction bands, show significant similarities. However, there are also some differences between them, such as the position of the valence band tops and conduction band bottoms, due to differences in structure. Also, the differences in crystal structure make the two kinds of  $VS_2$  have different applications, such as photodetectors or infrared sensors, due to their absorption in the infrared light region.

## References

- [1] Reber J F, Meier K. Photochemical production of hydrogen with zinc sulfide suspensions [J]. *Journal of Physical Chemistry*, 1984, (88:24): 5903-5913.
- [2] Hernández-Gordillo A, Tzompantzi F, Gámez R. An efficient ZnS-UV photocatalysts generated in situ from ZnS(en) 0.5 hybrid during the H<sub>2</sub> production in methanol–water solution [J]. *International Journal of Hydrogen Energy*, 2012, (37): 17002-17008.
- [3] Jin-Song H, Ling-Ling R, Yu-Guo G, Han-Pu L, An-Min C, Li-Jun W, Chun-Li B. Mass production and high photocatalytic activity of ZnS nanoporous nanoparticles [J]. *Angewandte Chemie*, 2010, (44): 1269-1273.
- [4] Clark S J, Segall M D, Pickard C J, Hasnip P J, Probert M I J, Refson K, Payne M C. First principles methods using CASTEP [J]. *Zeitschrift fuer Kristallographie*, 2005, (220): 567-570
- [5] Perdew J P, Ruzsinszky A, Csonka G I, Vydrov O A, Scuseria G E, Constant-in L A, Zhou X, Burke K. Generalized gradient approximation for solids and their surfaces [J]. *Physics*, 2007, (32): 22-28.
- [6] Pfrommer B G, Co?T?é M, Louie S G, Cohen M L. Ab initio study of silicon in the R8 phase [J]. *Physical Review B*, 1997, (56): 6662-6668.